Frequency-Domain based Single-Carrier Waveform Design through Precoder

Fumiyuki Adachi* and Amnart Boonkajay†
Department of Communications Engineering, Graduate School of Engineering, Tohoku University
6-6-05 Aza-Aoba, Aramaki, Aoba-ku, Sendai, Miyagi, 980-8579 Japan
Email: * adachi@ecei.tohoku.ac.jp, †amnart@mobile.ecei.tohoku.ac.jp

Abstract— **There are two types of signal waveform: single-carrier (SC) and multi-carrier (MC). A representative of MC signal is orthogonal frequency division multiplexing (OFDM). SC signal can be considered as a linear precoded OFDM signal and has lower peak-to-average power ratio (PAPR) than OFDM signal. There exist many variants between SC and MC signals depending on the linear precoder. The linear precoder can be designed to generate a SC signal having very-low-PAPR based on the minimum variance of instantaneous transmit power (VIP) criterion, or can be extended to generate SC spread spectrum (SS) signal. The frequency-domain based precoder design is presented and a tradeoff between PAPR and bit-error rate (BER) is discussed in this paper.**

Keywords— Single-carrier (SC) transmission, spread spectrum (SS), frequency-domain equalization (FDE), peak-to-average power ratio (PAPR)

I. INTRODUCTION

Multi-carrier (MC) signal transmission [1], such as orthogonal frequency division multiplexing (OFDM), is robust against frequency-selective fading [2], but its high peak-to-average power ratio (PAPR) is the main drawback. On the other hand, single-carrier (SC) transmission [3] is attractive for uplink communication because of its lower PAPR. The use of frequency-domain equalization (FDE) can take advantage of the channel frequency selectivity to improve the bit-error rate (BER) performance of SC transmission [4].

OFDM signal can be generated by using inverse discrete Fourier transform (IDFT) [5]. The time-domain based generation of SC signal has being used for long time. Recently, however, SC signal generation in frequency-domain has gained much attention; SC signal can be generated by inserting DFT as a linear precoder before IDFT of OFDM transmitter [6-8]. Because of precoder, the subcarriers (we use this terminology for the ease of explanation) of SC are correlated while those of OFDM are independent. This can be considered as the reason of low-PAPR property of SC.

SC and OFDM signals are considered as two extreme cases. Many low-PAPR variations of SC signal waveform exist between SC and OFDM, where the precoder takes an important role to generate low-PAPR SC signal waveforms. The linear precoder can be a combination of DFT and transmit filter implemented in the frequency domain. Among various transmit filters, square-root Nyquist filter with roll-off factor of higher than 0.5 provides a sufficiently low-PAPR SC signal [9, 10]. Moreover, low-PAPR SC signals can also be generated [11] based on the minimum variance of instantaneous transmit power (min-VIP) criterion [6]. The use of transmit filter can take an advantage of bandwidth expansion. Joint MMSE-FDE and spectrum combining [12] can be employed at the receiver to obtain additional frequency diversity gain. However, since the bandwidth expansion ratio is limited to two, the achievable frequency diversity gain is limited. It is shown in this paper that a tradeoff among PAPR, spectrum efficiency (SE), and BER depends on the precoder design.

Spread spectrum (SS) technique provides increased frequency diversity gain, but at the cost of SE. In this paper, it is shown that the linear precoder which performs frequency-domain spreading and mapping can be designed. This is called SC with frequency-domain SS (SC-FDSS) [13]. Joint MMSE-FDE and spectrum combining [12] can be employed as the de-spreading technique. There is also a tradeoff among PAPR, SE, and BER similar to the non-spreading SC case. To improve SE, SS can be combined with multi-access, i.e., code-division multi-access (CDMA) [14]. The combination of SC-FDSS and CDMA is expected to provide good BER-PAPR tradeoff among two conventional types of CDMA: direct-sequence CDMA (DS-CDMA) [e.g., 15] and OFDM-CDMA [16]. In addition, rake combining can be replaced by FDE to improve the BER performance of DS-CDMA [17].

The rest of this paper is organized as follows. In Section II, the role of linear precoder is discussed. Section III introduces the precoder design based on min-VIP criterion for of SC-FDE and its BER-PAPR tradeoff. Section IV introduces the transceiver design of SC-FDSS and its performance. Section V concludes the paper.

II. RELATIONSHIP BETWEEN SC AND OFDM

The SC signal is equivalent to precoded OFDM signal [8]. The transmitter structure to generate SC and OFDM signals is illustrated in Fig. 1.

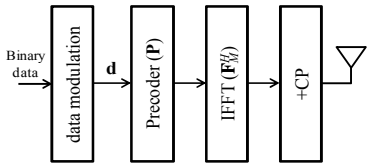

Fig. 1. Transmitter structure to generate SC and MC signals.

When $\mathbf{P}=\mathbf{I}$ (identity matrix of size M-by-M), OFDM signal $\mathbf{s}_{\mathrm{OFDM}}=[s_{\mathrm{OFDM}}(0),s_{\mathrm{OFDM}}(1),\ldots,s_{\mathrm{OFDM}}(M-1)]^{\mathrm{T}}$ is generated as

$$\mathbf{s}_{\mathrm{OFDM}} = \mathbf{F}_M^H \mathbf{d}\,, \tag{1}$$

where $\mathbf{d}=[d(0),d(1),\ldots,d(M-1)]^T$ represents the transmit symbol block and $\mathbf{F}_M^H$ denotes the IDFT matrix given by

$$\mathbf{F}_M^H = \frac{1}{\sqrt{M}}\begin{bmatrix} 1 & 1 & \cdots & 1 \\ 1 & e^{\frac{j2\pi(1)(1)}{M}} & \cdots & e^{\frac{j2\pi(1)(M-1)}{M}} \\ \vdots & \vdots & \ddots & \vdots \\ 1 & e^{\frac{j2\pi(M-1)(1)}{M}} & \cdots & e^{\frac{j2\pi(M-1)(M-1)}{M}} \end{bmatrix}. \tag{2}$$

When $\mathbf{P}=\mathbf{F}_M$ (DFT matrix of size M-by-M), the SC signal $\mathbf{s}_{\mathrm{SC}}=[s_{\mathrm{SC}}(0),s_{\mathrm{SC}}(1),\ldots,s_{\mathrm{SC}}(M-1)]^{\mathrm{T}}=\mathbf{d}$ is generated as [6-8]

$$\mathbf{s}_{SC} = \mathbf{F}_M^H \mathbf{P}\mathbf{d} = \mathbf{d}\,. \tag{3}$$

Any low PAPR SC signal variant between SC and OFDM can be generated by introducing the frequency-domain filter (or mapping) $\mathbf{W}$ into $\mathbf{P}$ as

$$\mathbf{P} = \mathbf{W}\mathbf{F}_M\,. \tag{4}$$

The design of precoder $\mathbf{P}$ for reducing the PAPR of SC signal is found in [6, 7]. Note that precoded OFDM considered in [6, 7] is a family of SC signal. In [7], the precoder of size larger than M (i.e., transmit signal bandwidth is wider than the original signal bandwidth) is studied. The use of square-root Nyquist filter [9-10, 18] is one good example for SC [9], in which $\mathbf{W}$ is a diagonal matrix containing the filter transfer function.

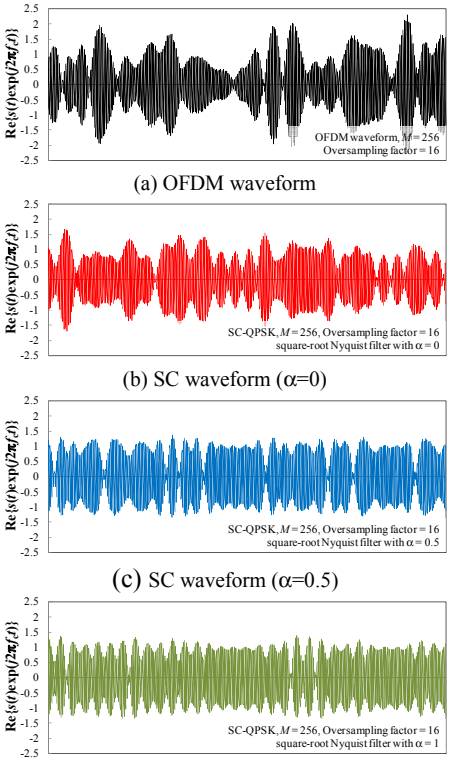

(a) OFDM waveform

(b) SC waveform (α=0)

(c) SC waveform (α=0.5)

(d) SC waveform (α=1)

Fig. 2. Comparison of SC and OFDM waveforms when M=256.

Figure 2 compares the square-root Nyquist filtered SC signal waveforms for different values of filter roll-off factor α to OFDM signal waveform with M=256 symbols. It is seen that the use of larger α exhibits better PAPR suppression at the cost of the bandwidth expansion by a factor of 1+α. Joint MMSE-FDE and spectrum combining [12] can be used to improve the BER performance by taking advantage of bandwidth expansion. However, since the maximum bandwidth expansion is limited to two, the BER performance improvement is limited. This brings us to introduce the SS transmission to further improve the BER performance.

In the following sections, we will design the transmit filter $\mathbf{W}$ based on the min-VIP criterion [6, 9]. Then, we will design the transmit filter $\mathbf{W}$ to generate the SC-FDSS signals [13].

III. Low-PAPR SC Signal Design

SC signal is generally a low-PAPR signal; however, its PAPR may increase when a particular precoder is applied. We use the min-VIP criterion (which has been introduced in [6] for OFDM signal) to determine the frequency-domain filter $\mathbf{W}$ of (4) in order to reduce the PAPR of SC signals.

A. Signal Representation

We assume a single-user SC-FDE block transmission of M data-modulated symbols over N_c subcarriers (assuming N_c=2M for simplicity). The transmitter and receiver structure is illustrated in Fig. 3.

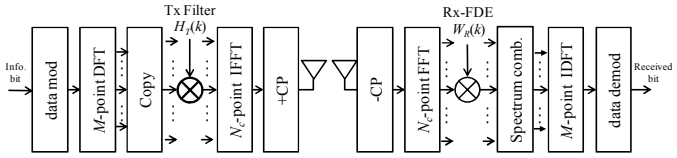

Fig. 3. Transmitter and receiver structure of SC-FDE using low-PAPR transmit filtering.

Decomposing the precoder $\mathbf{P}$ as $\mathbf{P}=\mathbf{H}_T\mathbf{E}_M$, the SC signal $\mathbf{s}=[s(0),s(1),\ldots,s(N_c-1)]^{\mathrm{T}}$ can be expressed as

$$\mathbf{s} = \mathbf{F}_{N_c}^H \mathbf{H}_T \mathbf{E}_M \mathbf{d}\,, \tag{5}$$

where $\mathbf{H}_T$ is an $N_c\times N_c$ diagonal matrix representing transmit filter given by

$$\mathbf{H}_T = diag\left[0,\ldots,H_T\left(\frac{N_c-J}{2}\right),\ldots,H_T\left(\frac{N_c+J}{2}-1\right),\ldots,0\right] \tag{6}$$

with J=(1+α)M and $\mathbf{E}_M$ is a row-repeated version of $\mathbf{F}_M$, which is given by

$$\mathbf{E}_M = \left[\mathbf{f}_M^T\left(\frac{M}{2}\right)\cdots\mathbf{f}_M^T(M-1)\cdots\mathbf{f}_M^T(0)\cdots\mathbf{f}_M^T(M-1)\cdots\mathbf{f}_M^T(0)\cdots\mathbf{f}_M^T\left(\frac{M}{2}-1\right)\right]^T, \tag{7}$$

with $\mathbf{f}_M(m)$ being the m-th row of $\mathbf{F}_M$. The determination of filter coefficient $H_T(k)$ will be described in Sect. III-B. Finally, the cyclic-prefix (CP)-inserted signal block is transmitted.

The transmitted signal goes through an L-path independent symbol-spaced block Rayleigh fading channel [2]. The received signal $\mathbf{r}=[r(0),r(1),\ldots,r(N_c-1)]^T$ after CP removal is represented in the time-domain as

$$\mathbf{r} = \sqrt{2E_s/T_s}\,\mathbf{h}\mathbf{s} + \mathbf{n}\,, \tag{8}$$

where E_s and T_s are the symbol energy and the symbol duration, respectively. $\mathbf{n}$ is the additive white Gaussian noise (AWGN) vector with each element representing independent and identically distributed (i.i.d.) zero-mean complex Gaussian variable having the variance $2N_0/T_s$ (N_0 is the one-sided noise power spectrum density). The channel matrix $\mathbf{h}$ is a circular matrix and is given as

$$\mathbf{h}=\begin{bmatrix} h_0 & & & h_{L-1} & \cdots & h_1 \\ h_1 & \ddots & & & \ddots & \vdots \\ \vdots & & h_0 & \mathbf{0} & & h_{L-1} \\ h_{L-1} & & h_1 & \ddots & & \\ & \ddots & \vdots & & \ddots & \\ \mathbf{0} & & h_{L-1} & \cdots & \cdots & h_0 \end{bmatrix}, \tag{9}$$

where h_l is the complex-valued path gain of the l-th path. The received signal $\mathbf{r}$ is transformed into the frequency-domain signal $\mathbf{R}$ by N_c-point fast Fourier transform (FFT) as

$$\begin{aligned}\mathbf{R}&=\sqrt{2E_s/T_s}\mathbf{F}_{N_c}\mathbf{h}\mathbf{F}_{N_c}^H\mathbf{H}_T\mathbf{D}+\mathbf{F}_{N_c}\mathbf{n}\\&=\sqrt{2E_s/T_s}\mathbf{H}_c\mathbf{H}_T\mathbf{D}+\mathbf{N}\end{aligned}, \tag{10}$$

where $\mathbf{H}_c=\mathbf{F}_{N_c}\mathbf{h}\mathbf{F}_{N_c}^H=diag[H_c(0),...,H_c(N_c-1)]$ and $\mathbf{D}=\mathbf{E}_M\mathbf{d}$ is the frequency-domain signal of $2M$ subcarriers, which is obtained by copying the frequency components of original M-symbol transmit signal.

The weight matrix $\mathbf{W}_R$ of size of $M\times N_c$ for joint MMSE-FDE and spectrum combining is given as [12]

$$\mathbf{W}_R=\begin{bmatrix} & & W_R(\frac{N_c}{4}) & & & W_R(\frac{3N_c}{4}-1) & \\ & \mathbf{0} & & & & \ddots & \\ & & & & & & W_R(N_c-1) \\ W_R(0) & & & \ddots & & & \\ & \ddots & & & & \mathbf{0} & \\ & & W_R(\frac{N_c}{4}-1) & & W_R(\frac{3N_c}{4}-1) & & \end{bmatrix} \tag{11}$$

with

$$W_R(k)=\frac{H_c^*(k)H_T^*(k)}{\sum_{g=0}^{1}\left|H_c(k\bmod M+gM)H_T(k\bmod M+gM)\right|^2+(E_s/N_0)^{-1}}. \tag{12}$$

The frequency-domain received signal $\mathbf{W}_R\mathbf{R}$ after joint MMSE-FDE and spectrum combining is transformed by M-point IDFT back into the time-domain received signal $\hat{\mathbf{d}}=[\hat{d}(0),\hat{d}(1),\ldots,\hat{d}(M-1)]^T$ as

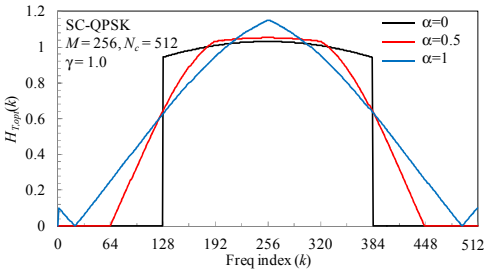

Fig. 4. Low-PAPR filter based on min-VIP criterion.

$$\hat{\mathbf{d}}=\mathbf{F}_M^H\mathbf{W}_R\mathbf{R}. \tag{13}$$

B. Low PAPR Transmit Filter Design

The frequency-domain transmit filter $\mathbf{H}_T$ is determined so as to minimize the VIP. Firstly, the VIP value σ^2 is determined from the time-domain transmit signal $\mathbf{s}$ as [6]

$$\begin{aligned}\sigma^2&=\frac{1}{N_c}\sum_{n=0}^{N_c-1}E\left[\left||s(n)|^2-E[|s(n)|^2]\right|^2\right]\\&=\frac{1}{N_c}\sum_{n=0}^{N_c-1}E[|s(n)|^4]-P_{avg}^2\end{aligned}, \tag{14}$$

where P_{avg} is the average transmit power. By assuming that all transmit symbols are i.i.d. and introducing $\mathbf{X}=\mathbf{F}_{N_c}^H\mathbf{H}_T\mathbf{E}_M$, (14) can be rewritten as

$$\sigma^2=\frac{1}{N_c}\sum_{n=0}^{N_c-1}\left[2\left[\sum_{m=0}^{M-1}|x_{nm}|^2\right]^2-(2-\kappa)\sum_{m=0}^{M-1}|x_{nm}|^4\right]-P_{avg}^2, \tag{15}$$

where $\kappa=E[|d(m)|^4]$ and x_{nm} represents the (n, m)-th element of $\mathbf{X}$ and is a function of $H_T(k)$ which is determined based on the min-VIP criterion as

$$\begin{aligned}&\arg\min_{\{H_T(k)\}}\sigma^2\\&\text{s.t. }\frac{1}{M}\sum_{k=0}^{N_c-1}|H_T(k)|^2=1, H_T(k)\ge 0\ \forall k\end{aligned}, \tag{16}$$

which can be solved via iterative gradient search method [19].

The derived filter transfer function $\{H_T(k);\ k=0\sim M-1\}$ for M=256 and QPSK modulation is shown in Fig. 4. It should be noted that the filter depends on the modulation type and that the complexity of transceiver remains the same as that of square-root Nyquist filtered SC-FDE.

C. Performance Comparison

A block transmission of M=256 symbols and N_c=512 subcarriers is considered. As for data modulation, QPSK and 16-QAM are considered. The propagation channel is assumed to be a frequency-selective block Rayleigh fading channel having symbol-spaced L=16-path uniform power-delay profile. Ideal channel estimation is assumed. BER and PAPR of SC-FDE using min-VIP based low-PAPR transmit filter are compared with square-root Nyquist filtered SC-FDE.

Figure 5 plots the QPSK-modulated transmit SC signal waveforms using square-root Nyquist filter and the min-VIP based low-PAPR filter. It is seen that the peak power of SC signal waveform based on min-VIP criterion is not much different from square-root Nyquist filtered SC waveform when $\alpha<0.5$, but clear peak power reduction is seen when $\alpha=1$. PAPR reduction is about 0.3 dB when $\alpha<0.5$ and is as much as 1.3 dB when $\alpha=1$.

The BER performance and PAPR distribution were measured. Then, $PAPR_{0.1\%}$ and the average received signal energy per bit-to-noise power spectrum density ratio $E_b/N_0=(1/N_{mod})(E_s/N_0)(1+N_g/N_c)$ required for BER=0.001 are obtained to find the BER-PAPR tradeoff. $PAPR_{0.1\%}$ represents the PAPR value which the PAPR exceeds at a probability of

0.1%. N_{mod} is the modulation level (N_{mod}=2 for QPSK and 4 for 16-QAM). Fig. 6 plots the BER-PAPR tradeoff. It can be seen that the min-VIP based filter design provides lower PAPR than the square-root Nyquist filter when α>0.5 while achieving almost the same E_b/N_0 required for achieving BER=0.001.

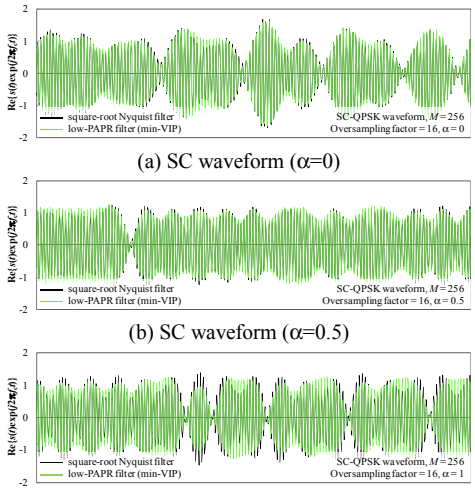

(a) SC waveform (α=0)

(b) SC waveform (α=0.5)

(c) SC waveform (α=1)

Fig. 5. Comparison of SC waveforms.

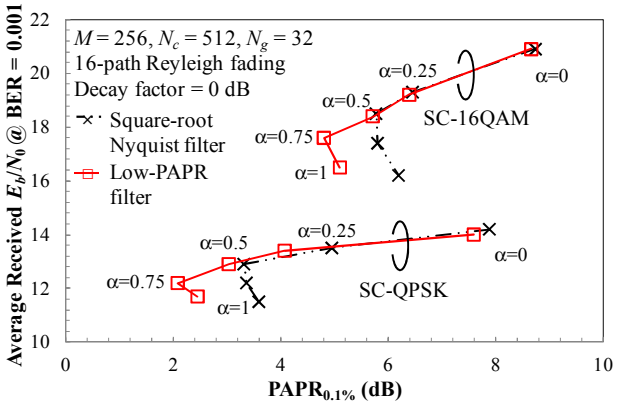

Fig. 6. BER-PAPR tradeoff of SC-FDE.

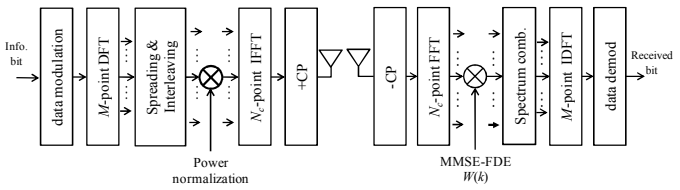

Fig. 7. Transmitter and receiver structure for SC-FDSS.

IV. Frequency-Domain Spread SC Signal Design

The maximum bandwidth expansion ratio achievable by using the frequency-domain filter **W** in the precoder **P** (=**WF**$_M$) is limited to 2 [6-7, 9, 11-12]. Below, we consider more than two times bandwidth expansion. This is done through SS process. We will extend the design of frequency-domain filter **W** to generate SS signal. Below, a single-user block transmission of M data-modulated symbols over N_c subcarriers is assumed, i.e., the spreading factor is SF=N_c/M. Joint MMSE-FDE and spectrum combining [12] can also be used as the de-spreader at the receiver. The transmitter and receiver structure for SC-FDSS is illustrated in Fig. 7.

A. Signal Representation

Similar to Sect. III, the SC-FDSS signal $\mathbf{s}=[s(0),s(1),...,s(N_c-1)]^T$ can be generated by modifying the frequency-domain filter **C** (note that notation **C** is used instead of **W**, i.e., the precoder of (4) becomes $\mathbf{P}=\mathbf{CF}_M$) as

$$\mathbf{C}=\frac{1}{\sqrt{SF}}\begin{bmatrix} C(0) & & \\ & \ddots & \\ & & C(SF-1) \\ & \vdots & \\ C(0) & & \\ & \ddots & \\ & & C(SF-1) \end{bmatrix}_{N_c\times M}, \quad (17)$$

where $C(k)$ has unit-magnitude (i.e. $|C(k)|^2$=1 for all k). Below, $C(k)$ =1 is assumed for all k for simplicity. It is understood from Fig. 7 that SC-FDSS transmitter requires DFT operation, which is not needed in OFDM-CDMA (note that both DFT and IFFT are not required in DS-CDMA transmitter) and therefore, the complexity of SC-FDSS transceiver is slightly higher. However, SC-FDSS transmitter is similar to the transmitter of SC with frequency-domain multi-access (SC-FDMA) [20].

The transmitted signal goes through a chip-space L-path frequency-selective block fading channel. The N_c-chip received signal $\mathbf{r}=\sqrt{2E_s/T_s}\mathbf{hs}+\mathbf{n}$ is transformed by N_c-point FFT into frequency domain signal **R** as

$$\begin{aligned}\mathbf{R} &= \sqrt{2E_s/T_s}\mathbf{F}_{N_c}\mathbf{hs}+\mathbf{F}_{N_c}\mathbf{n} \\ &= \sqrt{2E_s/T_s}\mathbf{F}_{N_c}\mathbf{hF}_{N_c}^H\mathbf{CD}+\mathbf{F}_{N_c}\mathbf{n}, \\ &= \sqrt{2E_s/T_s}\mathbf{H}_c\mathbf{CD}+\mathbf{N}\end{aligned} \quad (18)$$

where $\mathbf{H}_c=\mathbf{F}_{N_c}\mathbf{hF}_{N_c}^H=diag[H_c(0),...,H_c(N_c-1)]$ and **D**=**F**$_M$**d** is frequency-domain transmit signal before spreading.

De-spreading at the receiver is done by joint MMSE-FDE and spectrum combining [12], which is described by $\mathbf{W}_R$ of size $M\times N_c$ as

$$\mathbf{W}_R=[\mathbf{W}_{R,0}\ \mathbf{W}_{R,1}\cdots\mathbf{W}_{R,SF-1}]_{M\times N_c} \quad (19)$$

with

$$\mathbf{W}_{R,n}=diag[W_R(\tfrac{(nSF)}{SF}M),W_R(\tfrac{(nSF)}{SF}M+1),\ldots,W_R(\tfrac{((n+1)SF)}{SF}M-1)], \quad (20)$$

where $W_R(k)$, k=0~N_c-1, is the weight that minimizes the mean-square error (MSE) between the frequency-domain signal **D** before spreading and the frequency-domain received signal $\hat{\mathbf{D}}=\mathbf{W}_R\mathbf{R}$ after de-spreading. $W_R(k)$ is given by

$$W_R(k)=\frac{H_c^*(k)C^*(k)}{\sum_{g=0}^{SF-1}\left|H_c(k\bmod M+gM)C(k\bmod M+gM)\right|^2+\left(\frac{E_s}{N_0}\right)^{-1}}. \quad (21)$$

The frequency-domain signal $\hat{\mathbf{D}}$ after joint MMSE-FDE and spectrum combining is finally transformed by M-point IDFT back into time-domain signal $\hat{\mathbf{d}} = [\hat{d}(0), \hat{d}(1), ..., \hat{d}(M-1)]^T$ as

$$\hat{\mathbf{d}} = \mathbf{F}_M^H \hat{\mathbf{D}} . \quad (22)$$

B. Performance Comparison

A block transmission of SC-FDSS signal with N_c=256 subcarriers is considered. The propagation channel is assumed to be a frequency-selective block Rayleigh fading channel having chip-spaced L=16-path uniform power-delay profile. BER-PAPR tradeoff is evaluated and is compared with direct-sequence SS (DS-SS) and MC-SS.

Figure 8 compares the BER-PAPR tradeoffs of DS-SS, MC-SS, and SC-FDSS. Overall, SC-FDSS achieves BER-PAPR tradeoff better than both DS-SS and MC-SS. It is seen from Fig. 8 that SC-FDSS achieves better BER performance than both DS-SS and MC-SS. Performance improvement in SC-FDSS is due to larger frequency-diversity gain through joint MMSE-FDE and spectrum combining. It is interesting to note that PAPR is minimized when SF=2 for SC-FDSS. This is because of the interleaving property in time-domain signal of SC-FDSS, which reduces the peak caused by pulse overlapping when SF<4 [10].

However, PAPR of SC-FDSS is larger than DS-SS when SF=8, indicating that some PAPR reduction scheme should be employed. A combination of SC-FDSS and min-VIP based precoder design, as described in Sect. III, can be a good approach. This can be left as our future study.

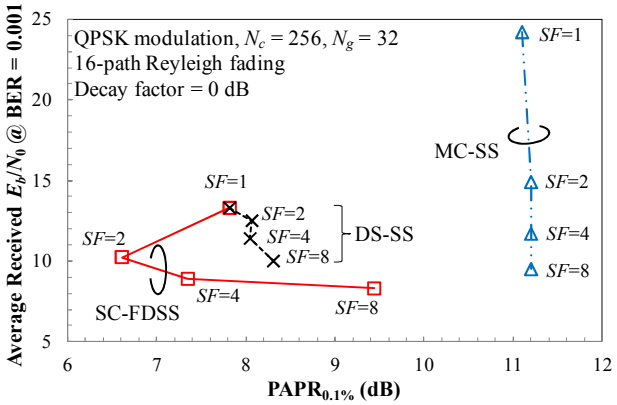

Fig. 8. BER-PAPR tradeoff of SC-FDSS.

V. Conclusion

The relationship between SC and OFDM signal waveforms can be described by using the precoder. The PAPR of the SC signal waveform can be controlled by the precoder. There exists the trade-off between PAPR and BER. Precoder design based on min-VIP criterion was presented. Also precoder was extended to include more than two times bandwidth expansion (i.e., spread spectrum). It was confirmed that a good PAPR-BER tradeoff can be achieved for both the non-spreading and spreading cases.

References

[1] S. H. Han and J. H. Lee, "An Overview of Peak-to-Average Power Ratio Reduction Techniques for Multicarrier Transmission," *IEEE Trans. Wireless Commun.*, vol. 12, no. 2, pp. 56-65, April 2005.

[2] A. Goldsmith, *Wireless Communications*, Cambridge University Press, 2005.

[3] H. Sari, G. Karam, and I. Jeanclaude, "Transmission Techniques for Digital Terrestrial TV Broadcasting," *IEEE Commun. Mag.*, vol. 33, pp. 100-109, February 1995.

[4] D. Falconer, S. Ariyavisitakul, A. Benyamin-Seeyar, and B. Eidson, "Frequency Domain Equalization for Single-Carrier Broadband Wireless Systems," *IEEE Commun. Mag.*, vol. 40, no. 4, pp. 58-66, April 2002.

[5] M. Sternad, T. Ottosson, T. Ahlén, A. Svensson, and A. Brunström, "Towards Systems Beyond 3G based on Adaptive OFDMA Transmission," *Proc. IEEE*, vol. 95, no. 12, pp. 2432-2455, Dec. 2007.

[6] D. Falconer, "Linear Precoding of OFDMA, Signals to Minimize Their Instantaneous Power Variance," *IEEE Trans. Commun.*, vol. 59, no. 4, pp. 1154-1162, April 2011.

[7] S. Slimane, "Reducing the Peak-to-Average Power Ratio Of OFDM Signals Through Precodings," *IEEE Trans. Veh. Technol.*, vol. 56, no. 2, pp. 686-695, March 2007.

[8] F. Adachi, K. Takeda, and H. Tomeba, "Introduction of Frequency-Domain Signal Processing to Broadband Single-Carrier Transmissions in a Wireless Channel," *IEICE Trans. Commun.*, vol. E92-B, no. 9, pp. 2789-2808, Sept. 2009.

[9] S. Okuyama, K. Takeda, and F. Adachi, "MMSE Frequency-domain Equalization Using Spectrum Combining for Nyquist Filtered Broadband Single-Carrier Transmission," *Proc. 71st IEEE Vehicular Technology Conference (VTC 2010-Spring)*, Taipei, Taiwan, 16-19 May 2010.

[10] S. Daumont, B. Rihawi, and Y. Lout, "Root-Raised Cosine Filter Influences on PAPR Distribution of Single Carrier Signals," *Proc. The 3rd International Symposium on Communications, Control and Signal Processing (ISCCSP 2008)*, pp. 841-845, Malta, 12-14 March 2008.

[11] A. Boonkajay, T. Obara, T. Yamamoto, and F. Adachi, "Performance Evaluation of Low-PAPR Transmit Filter for Single-Carrier Transmission," *Proc. The 18th Asia-Pacific Conference on Communications (APCC 2012)*, Jeju Island, Korea, 15-17 Oct. 2012.

[12] T. Obara, K. Takeda, and F. Adachi, "Joint Frequency-Domain Equalization and Spectrum Combining for the Reception of SC Signals in the Presence of Timing Offset," *Proc. The 71st IEEE Vehicular Technology Conference (VTC 2010-Spring)*, Taipei, Taiwan, 16-19 May 2010.

[13] A. Boonkajay, T. Obara, T. Yamamoto, and F. Adachi, "Frequency-Domain Single-Carrier Spread Spectrum with Joint FDE and Spectrum Combining," *Proc. The 9th International Conference on Information, Communications and Signal Processing (ICICS 2013),* Tainan, Taiwan, 10-13 Dec. 2013.

[14] A. J. Viterbi, *CDMA, Principles of Spread Spectrum Communications*, Addison-Wesley, 1995.

[15] F. Adachi, M. Sawahashi, and H. Suda, "Wideband DS-CDMA for next generation mobile communications systems," *IEEE Commun. Mag.*, vol. 36, no. 9, pp. 56-69, Sept. 1998.

[16] S. Hara, and R. Prasad, "Overview of Multicarrier CDMA", *IEEE Commun. Mag.*, vol. 35, pp. 126-133, Dec. 1997.

[17] F. Adachi, T. Sao, and T. Itagaki, "Performance of multicode DS-CDMA using frequency domain equalization in a frequency selective fading channel," *IEE Electron. Lett.*, vol. 39, no.2, pp. 239-241, Jan. 2003.

[18] Y. Akaiwa, *Introduction to Digital Mobile Communication*, 1st ed., Wiley, 1997.

[19] S. Boyd, and L. Vandenberghe, *Convex Optimization*, Cambridge University Press, 2004.

[20] H. G. Myung, J. Lim, and D. Goodman, "Single Carrier FDMA for Uplink Wireless Transmission," *IEEE Veh. Technol. Mag.*, vol. 1, no. 3, pp. 30-38, Sept. 2006.

APPENDIX

Fig. A-1 plots the BER and PAPR performances of filtered SC-FDE using square-root Nyquist filter and the min-VIP based low-PAPR filter for QPSK modulation. It is seen that the min-VIP based low-PAPR filter achieves very similar BER performance to square-root Nyquist filter when α=0 and 0.5 while only a slight degradation is seen when α=1.

Fig. A-2 plots the complementary cumulative distribution function (CCDF) of PAPR for QPSK modulation. It is clearly seen that the min-VIP based low-PAPR filter achieves lower PAPR than square-root Nyquist filter for all values of α. PAPR reduction is pronounced when α>0.5.

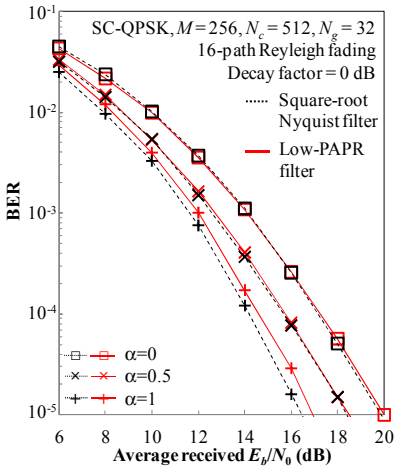

Fig. A-1. BER performance of filtered SC-FDE.

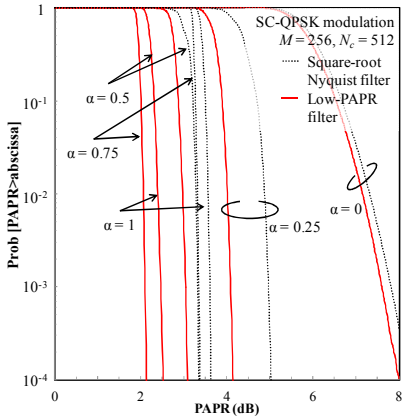

Fig. A-2. PAPR performance of filtered SC-FDE.

We also provide the BER and PAPR performance comparison of SS signals (i.e., DS-SS, MC-SS, and SC-FDSS). It is seen from Fig. A-3(a) and A-3(b) that SC-FDSS achieve better BER performance than both DS-SS and MC-SS. Performance improvement in SC-FDSS is achieved by joint MMSE-FDE and spectrum combining. In addition, it is also observed that MC-SS provides worse BER performance than SC-FDSS and DS-SS when SF≤4 due to lower frequency diversity gain.

Fig. A-4 shows the CCDF of PAPR of DS-SS, MC-SS, and SC-FDSS when SF≤8. PAPR slightly increases when SF increases in DS-SS. However, it is noticed that PAPR is minimized when SF=2 in SC-FDSS. This is because of the interleaving property in time-domain signal of the proposed SC-FDSS, which decreases the peak occurred from pulse overlapping when SF<4 [10]. However, PAPR increases when the interval between each time-domain non-zero signal is excessively wide. In addition, PAPR of SC-FDSS at SF=8 is still lower than MC-SS signal at SF=2 and 4.

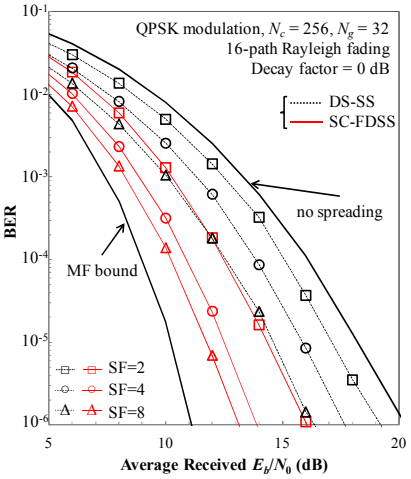

(a) SC-FDSS vs DS-SS

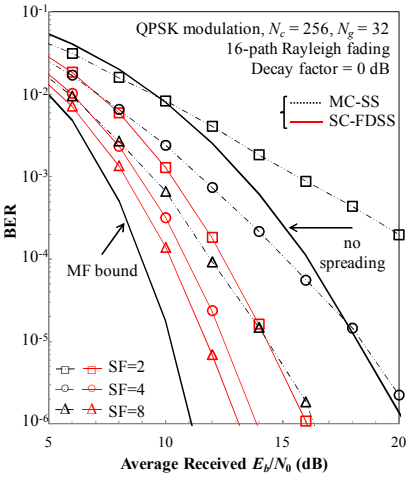

(b) SC-FDSS vs MC-SS

Fig. A-3. BER performances of SS transmission.

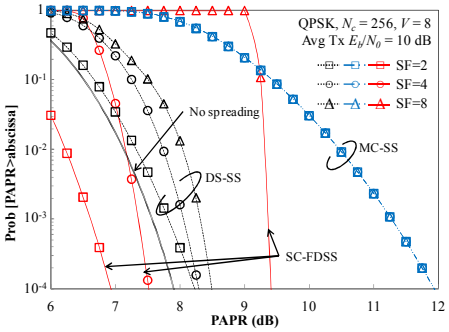

Fig. A-4. PAPR performances of SS signals.